

# Altitude effects of localized source currents on magnetotelluric responses

Shinya Sato

Graduate School of Engineering, Kyoto University

Email: [sato.shinya.27s@st.kyoto-u.ac.jp](mailto:sato.shinya.27s@st.kyoto-u.ac.jp)

## Abstract

The effects of localized source currents on Earth's magnetotelluric (MT) responses have been evaluated in terms of the changes in period and subsurface structure. The focus is on the bias within the MT responses arising from variations in altitude of the source current. The MT responses at 20 and 200 s are calculated at various vertical distances of the source current. A slight change in the source's altitude causes a shift in the MT responses, and the bias is large especially over the vertical distances explored in the MT data analysis (i.e., 100–150 km). This shift due to the source field should be considered in a real-data analysis because the distribution of conductivity with altitude in the ionosphere and the region controlling the ionospheric electrical process change temporally.

## Introduction

In magnetotelluric (MT) surveys, the primary electromagnetic fields arising from source fields are assumed horizontally uniform. The effects of localized source currents on the MT responses have been discussed in the literature (Madden and Nelson, 1964; Schmucker, 1970; Hermance and Peltier, 1970; Häkkinen et al., 1989; Pirjola, 1992), where impedances at long periods and at sites above structures of high resistivity are biased. For example, Pirjola (1992) reported that the apparent resistivity of 100  $\Omega\text{m}$  and at periods larger than 60 s were clearly affected. Their studies focused on period-dependent subsurface bias. However, the bias stemming from the variation in altitude of localized currents was not discussed in detail. In this study, the electromagnetic fields and MT responses were calculated by increasing the vertical distance of the source current (100, 105, ..., 595, and 600 km). The study revealed i) the numerical examples of the bias in the MT responses because of the variation in vertical distance of the source field, ii) implications from these examples, iii) the mathematical underpinning of this bias, and iv) the mathematical conditions for upholding the plane-wave assumption.

## Electromagnetic fields above Earth's surface

We chose a Cartesian coordinate system, where the  $x$ ,  $y$ , and  $z$  axes are northward, westward, and downward positive, respectively, with  $z = 0$  at Earth's surface. Ignoring the displacement current and using the SI system, Maxwell's equations in the frequency domain are

$$\nabla \times \mathbf{E} = -i\omega\mathbf{B}, \quad (1)$$

$$\nabla \times \mathbf{B} = \mu_0(\sigma\mathbf{E} + \mathbf{J}), \quad (2)$$

$$\nabla \cdot \mathbf{B} = 0, \quad (3)$$

where  $\mathbf{E}$ ,  $\mathbf{B}$ , and  $\mathbf{J}$  are the electric field, magnetic induction, and source current, respectively;  $\sigma$ ,  $\mu_0$ , and  $\omega$  are the electrical conductivity, the magnetic permeability of free space, and the angular frequency, respectively. Introducing the vector potential  $\mathbf{A}$  and the scalar potential  $\Pi$ , the electromagnetic fields are

$$\mathbf{B} = \nabla \times \mathbf{A}, \quad (4)$$

$$\mathbf{E} = -i\omega(\mathbf{A} + \nabla\Pi). \quad (5)$$

Applying the Lorenz gauge, the  $\mathbf{A}$  and the  $\Pi$  must satisfy

$$-\Delta\mathbf{A} + i\omega\sigma\mu_0\mathbf{A} = \mu_0\mathbf{J}, \quad (6)$$

$$i\omega\sigma\mu_0\Pi = -\nabla \cdot \mathbf{A}. \quad (7)$$

Considering the electromagnetic fields above Earth's surface (i.e.,  $z \leq 0$ ),  $\sigma$  may be taken as  $\sigma_0$  denoting the electrical conductivity of free space. As in Hermance and Peltier (1970), we consider a wire at an altitude  $z_1 < 0$  carrying an electric current  $I$ ; the current density is

$$\mathbf{J} = \begin{pmatrix} J_x \\ J_y \\ J_z \end{pmatrix} = I\delta(z - z_1)\delta(x) \begin{pmatrix} 0 \\ 1 \\ 0 \end{pmatrix}. \quad (8)$$

We focus on only  $A_y$ , the  $y$  component of  $\mathbf{A}$ , and  $\Pi$ . For this study, the horizontal Fourier transforms (FTs) are defined as

$$\tilde{F}(\eta, \zeta) = \int_{-\infty}^{\infty} \int_{-\infty}^{\infty} F(x, y) e^{i(\eta x + \zeta y)} dx dy, \quad (9)$$

$$F(x, y) = \frac{1}{4\pi^2} \int_{-\infty}^{\infty} \int_{-\infty}^{\infty} \tilde{F}(\eta, \zeta) e^{-i(\eta x + \zeta y)} d\eta d\zeta. \quad (10)$$

Eq. (10) enables us to transform Eq. (6) into

$$\frac{\partial}{\partial z^2} \tilde{A}_y - \beta_0^2 \tilde{A}_y = -\mu_0 \tilde{J}_y \quad (z \leq 0), \quad (11)$$

where  $\tilde{A}_y$  and  $\tilde{J}_y$  are  $A_y$  and  $J_y$  in the Fourier domain, respectively, and  $\beta_0 = \sqrt{(\eta^2 + \zeta^2) + i\omega\mu_0\sigma_0}$ . Eq. (11) is the Helmholtz equation and for which its Green's function satisfies

$$\frac{\partial}{\partial z^2} G(z, z') - \beta_0^2 G(z, z') = \delta(z - z'). \quad (12)$$

As shown in Arfken et al. (2012), the solution of  $G(z, z')$  is

$$G(z, z') = -\frac{(e^{-\beta_0|z-z'|} + \Lambda e^{-\beta_0|z+z'|})}{2\beta_0}, \quad (13)$$

where  $\Lambda$  is a constant required to uphold the boundary condition at  $z = 0$ . Consider a structure beneath Earth's surface ( $z > 0$ ) having a half-space of conductivity  $\sigma_1$ . The continuity of the electromagnetic fields parallel to the boundary yields

$$\Lambda(\eta, \zeta) = \frac{\beta_0 - \beta_1}{\beta_0 + \beta_1}, \quad (14)$$

where  $\beta_1 = \sqrt{(\eta^2 + \zeta^2) + i\omega\mu_0\sigma_1}$ . Applying the FT, Eq. (9),  $\tilde{J}_y$  in Eq. (11) becomes

$$\tilde{J}_y = 2\pi I \delta(z - z_1) \delta(\zeta). \quad (15)$$

Using Green's function, the solutions for  $\tilde{A}_y$  are

$$\tilde{A}_y = \pi \mu_0 I \frac{(e^{-\beta_0|z-z_1|} + \Lambda e^{-\beta_0|z+z_1|}) \delta(\zeta)}{\beta_0}. \quad (16)$$

Applying the inverse FT, Eq. (10), and considering  $\sigma_0 = 0$ ,  $A_y$  is written as

$$A_y = \frac{\mu_0 I}{4\pi} \int_{-\infty}^{\infty} \frac{(e^{-|\eta|(z-z_1)} + \Lambda(\eta, 0) e^{|\eta|(z+z_1)})}{|\eta|} e^{-i\eta x} d\eta \quad (z \leq 0). \quad (17)$$

The scalar potential is ignored because both sides in Eq. (7) are equal to zero. From Eqs. (4) and (5), the magnetic induction  $B_x$  and the electric field  $E_y$  at Earth's surface ( $z = 0$ ) is written as:

$$B_x = \frac{\mu_0 I}{2\pi} \int_{-\infty}^{\infty} \frac{\sqrt{\eta^2 + i\omega\mu_0\sigma_1}}{|\eta| + \sqrt{\eta^2 + i\omega\mu_0\sigma_1}} e^{|\eta|z_1} e^{-i\eta x} d\eta, \quad (18)$$

$$E_y = -i\omega \frac{\mu_0 I}{2\pi} \int_{-\infty}^{\infty} \frac{1}{|\eta| + \sqrt{\eta^2 + i\omega\mu_0\sigma_1}} e^{|\eta|z_1} e^{-i\eta x} d\eta. \quad (19)$$

Taking their ratio  $E_y/B_x$  gives the impedance  $Z_{yx}$ ,

$$Z_{yx} = \frac{-i\omega \int_{-\infty}^{\infty} \frac{1}{|\eta| + \sqrt{\eta^2 + i\omega\mu_0\sigma_1}} e^{|\eta|z_1} e^{-i\eta x} d\eta}{\int_{-\infty}^{\infty} \frac{\sqrt{\eta^2 + i\omega\mu_0\sigma_1}}{|\eta| + \sqrt{\eta^2 + i\omega\mu_0\sigma_1}} e^{|\eta|z_1} e^{-i\eta x} d\eta}. \quad (20)$$

For this study, the apparent resistivity  $\rho_{yx}$  is given by

$$\rho_{yx} = \frac{\mu_0}{2\pi f} |Z_{yx}|^2, \quad (21)$$

where  $Z_{yx}$  is defined in Eq. (20). Note that hereafter the distance unit used is “km” instead of “m” when stating horizontal/vertical distances ( $x, z_1$ ) although all the above values are calculating based on the SI system of units.

### MT responses biased by line current

Here, the subsurface resistivity and the time period is set to 1000  $\Omega\text{m}$  (i.e.,  $\sigma_1 = 10^{-3}$  S/m) and 20 s, respectively. The subsurface resistivity has the same value as that used for the crust in Hermance and Peltier (1970). By changing the altitude of the source current  $z_1$  from  $-100$  to  $-600$  km in increments of 5 km and the horizontal distance  $x$  ( $x = 1, 10, 100, 1000$  km), the variation in the field components  $B_x$  [Eq. (18)] and  $E_y$  [Eq. (19)], as well as impedance  $Z_{yx}$  [Eq. (20)] were determined. The integrals in Eqs. (18) and (19) were calculated using the discrete approximation; the convergence of each was verified. Note that the electric current  $I$  in Eq. (8) is 1000 A although the value has no influence on  $Z_{yx}$ . The calculated values of the apparent resistivity [Eq. (21)] and phase are shown in Fig. 1; their polarities of apparent for the magnetic amplitudes when  $x = 1$  km (black dots) are almost same as that for  $x = 10$  km (purple dots).

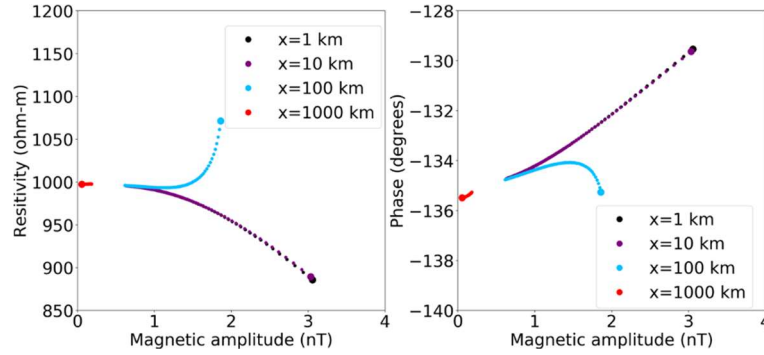


Figure 1. MT responses at a time period of 20 s: (left) Relationship between apparent resistivity and magnetic amplitude. The black/purple/light blue/red dots are the MT responses at horizontal distances of 1/10/100/1000 km from the source current. The largest dots mark calculations substituting  $-100$  km into  $z_1$ . The further from the largest dots by one point, the altitude increases by 5 km; (right) Relationship between phase and magnetic amplitude.

The polarities when  $x = 100$  or  $1000$  km (light blue/ red dots in Fig. 1) are different from the above two instances. Except for the horizontal distance of  $1000$  km, the MT responses are shifted largely depending on the vertical distance from the source current, particularly within the range  $100$ – $150$  km, where the MT responses have much different values from the subsurface resistivity of  $1000 \Omega\text{m}$ . Additionally, the MT responses at a time period of  $200$  s under the same conditions as the above were plotted (Fig. 2) and as expected, they are biased by the source current more than those of Fig. 1.

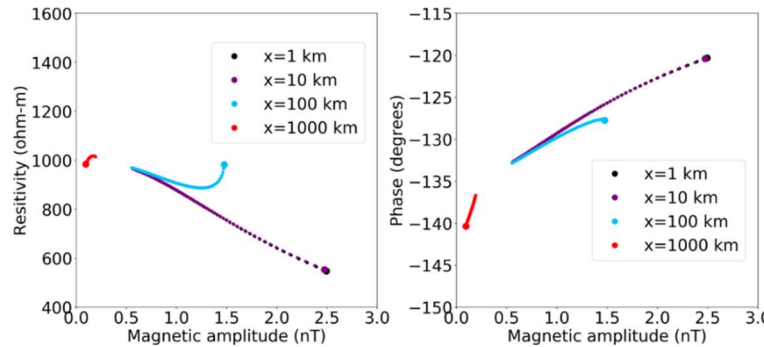


Figure 2. MT responses at a time period of 200 s.

## Discussion

A discussion is presented next of i) the mathematical basis of the bias on the MT responses due to the source field, ii) the mathematical condition upholding the plane-wave assumption, and iii) the implication arising from the numerical examples performed in this study.

The electromagnetic fields [Eqs. (18) and (19)] generated by the line current have an attenuation term

$$\alpha(\eta) = e^{|\eta|z_1}, \quad (22)$$

and a term conveying information regarding the subsurface structure

$$\beta(\eta) = \sqrt{\eta^2 + i\omega\mu_0\sigma_1}. \quad (23)$$

Substituting  $\frac{2\pi}{20}$  1/s,  $1.26 \cdot 10^{-6}$  H/m, and 0.001 S/m for  $\omega$ ,  $\mu_0$ , and  $\sigma_1$ , respectively, the apparent resistivity and phase are plotted (Fig. 1). When the wavenumber  $|\eta|$  is greater than  $2.0 \cdot 10^{-5}$ , the weight of  $\eta$  is greater than  $\omega\mu_0\sigma_1$ . When  $\alpha(\eta)$  in Eq. (22) is smaller than 0.01, the effect of  $|\eta|$  is assumed negligible. To uphold this assumption,  $|\eta|z_1$  should be smaller than  $-4.6$ , and when  $z_1 = -100$  km,  $|\eta|$  should be greater than  $4.6 \cdot 10^{-5}$ . Therefore, the integrands in Eqs. (18) and (19) are biased by wavenumber  $|\eta|$  at least within the interval  $2.0 \cdot 10^{-5} < |\eta| < 4.6 \cdot 10^{-5}$ . On the other hand, given that  $z_1 = -600$  km, the wavenumber effect is small enough to be negligible, and as a result, the apparent resistivity approaches a constant value of 1000  $\Omega\text{m}$ , i.e., the subsurface resistivity. As expected from the above discussion, the MT responses at 200 s are biased more than those at 20 s.

Both responses at 20 and 200 s have the same polarity; that is, they shift depending not only on the vertical ( $z_1$ ) but also on the horizontal distance ( $x$ ) between the site and the source current. The integrands in Eqs. (18) and (19) oscillate because of the factor  $e^{-i\eta x}$ , and substituting 1000 km into  $x$ , the apparent resistivity [Eq. (21)] at 20/200 s have values of 1000  $\Omega\text{m}$ . The mathematics behind these calculated results resides with the re-expressions of Eqs. (18) and (19),

$$B_x = \frac{\mu_0 I}{\pi} \int_0^\infty \frac{\sqrt{\eta^2 + ia}}{\eta + \sqrt{\eta^2 + ia}} (e^{\eta(z_1 - ix)} + e^{\eta(z_1 + ix)}) d\eta, \quad (24)$$

$$E_y = -i\omega \frac{\mu_0 I}{\pi} \int_0^\infty \frac{1}{\eta + \sqrt{\eta^2 + ia}} (e^{\eta(z_1 - ix)} + e^{\eta(z_1 + ix)}) d\eta, \quad (25)$$

where  $a = \omega\mu_0\sigma_1$ . Focusing on the term with  $e^{\eta(z_1 - ix)}$  and integrating by parts, we can obtain,

$$\int_0^\infty \frac{\sqrt{\eta^2 + ia}}{\eta + \sqrt{\eta^2 + ia}} e^{\eta(z_1 - ix)} d\eta = \frac{-1}{(z_1 + ix)} + \frac{-1}{\sqrt{ia}(z_1 + ix)^2} + \frac{-2}{ia(z_1 + ix)^3} \quad (26)$$

$$- \int_0^\infty \frac{d^3}{d\eta^3} \left( \frac{\sqrt{\eta^2 + ia}}{\eta + \sqrt{\eta^2 + ia}} \right) \frac{e^{\eta(z_1 - ix)}}{(z_1 - ix)^3} d\eta,$$

$$\int_0^\infty \frac{e^{\eta(z_1 - ix)}}{\eta + \sqrt{\eta^2 + ia}} d\eta = \frac{-1}{\sqrt{ia}(z_1 + ix)} + \frac{-1}{ia(z_1 + ix)^2} + \frac{-1}{(ia)^{\frac{3}{2}}(z_1 + ix)^3} - \int_0^\infty \frac{d^3}{d\eta^3} \left( \frac{1}{\eta + \sqrt{\eta^2 + ia}} \right) \frac{e^{\eta(z_1 - ix)}}{(z_1 - ix)^3} d\eta. \quad (27)$$

The triangle inequality and the inequality  $\left| \frac{1}{(\eta^2 + ia)} \right| \leq \frac{1}{a}$  ( $\eta \in \mathbb{R}$ ) enable the integrand of the last term

in Eq. (27) to be examined,

$$\left| \frac{d^3}{d\eta^3} \left( \frac{\sqrt{\eta^2 + ia}}{\eta + \sqrt{\eta^2 + ia}} \right) \right| = \left| \frac{3(\eta - \sqrt{\eta^2 + ia})}{(\eta + \sqrt{\eta^2 + ia})(\eta^2 + ia)^{\frac{3}{2}}} \left\{ 1 + \frac{\eta(\eta + 2\sqrt{\eta^2 + ia})}{(\eta^2 + ia)} \right\} \right| \quad (28)$$

$$\leq \frac{6\eta+3a}{a^2} \left(1 + \frac{3\eta^2+2\sqrt{a}\eta}{a}\right),$$

$$\left| \frac{d^3}{d\eta^3} \left( \frac{1}{\eta+\sqrt{\eta^2+ia}} \right) \right| = \left| \frac{-3\eta}{(\eta^2+ia)^{\frac{5}{2}}} \right| \leq \frac{3\eta}{a^2}. \quad (29)$$

Eqs. (28) and (29) and the inequality  $|\int_0^\infty F(\eta)d\eta| \leq \int_0^\infty |F(\eta)|d\eta$ , where  $F$  is an arbitrary function, give

$$\left| \int_0^\infty \frac{d^3}{d\eta^3} \left( \frac{\sqrt{\eta^2+ia}}{\eta+\sqrt{\eta^2+ia}} \right) e^{\eta(z_1-ix)} d\eta \right| \leq \int_0^\infty \frac{6\eta+3a}{a^2} \left(1 + \frac{3\eta^2+2\sqrt{a}\eta}{a}\right) e^{\eta z_1} d\eta, \quad (30)$$

$$\left| \int_0^\infty \frac{d^3}{d\eta^3} \left( \frac{1}{\eta+\sqrt{\eta^2+ia}} \right) e^{\eta(z_1-ix)} d\eta \right| \leq \int_0^\infty \frac{3\eta}{a^2} e^{\eta z_1} d\eta. \quad (31)$$

The right-hand sides of Eqs. (30) and (31) are constant and do not diverge. Replacing

$\int_0^\infty \frac{d^3}{d\eta^3} \left( \frac{\sqrt{\eta^2+ia}}{\eta+\sqrt{\eta^2+ia}} \right) e^{\eta(z_1-ix)} d\eta$  and  $\int_0^\infty \frac{d^3}{d\eta^3} \left( \frac{1}{\eta+\sqrt{\eta^2+ia}} \right) e^{\eta(z_1-ix)} d\eta$  with  $C_1$  and  $D_1$ , respectively,

the absolute values  $|C_1|$  and  $|D_1|$  are always less than a constant value. The same applies to

$\int_0^\infty \frac{\sqrt{\eta^2+ia}}{\eta+\sqrt{\eta^2+ia}} e^{\eta(z_1+ix)} d\eta$  and  $\int_0^\infty \frac{e^{\eta(z_1+ix)}}{\eta+\sqrt{\eta^2+ia}} d\eta$ , with  $\int_0^\infty \frac{d^3}{d\eta^3} \left( \frac{\sqrt{\eta^2+ia}}{\eta+\sqrt{\eta^2+ia}} \right) e^{\eta(z_1-ix)} d\eta$  and

$\int_0^\infty \frac{d^3}{d\eta^3} \left( \frac{1}{\eta+\sqrt{\eta^2+ia}} \right) e^{\eta(z_1-ix)} d\eta$  being replaced by  $C_2$  and  $D_2$ , respectively. As a result, the

electromagnetic fields take the form

$$B_x = -\frac{\mu_0 I}{\pi} \left\{ \frac{1}{(z_1+ix)} + \frac{1}{\sqrt{ia}(z_1+ix)^2} + \frac{2+iaC_1}{ia(z_1+ix)^3} + \frac{1}{(z_1-ix)} + \frac{1}{\sqrt{ia}(z_1-ix)^2} + \frac{2+iaC_2}{ia(z_1-ix)^3} \right\}, \quad (32)$$

$$E_y = i\omega \frac{\mu_0 I}{\pi} \left\{ \frac{1}{\sqrt{ia}(z_1+ix)} + \frac{1}{ia(z_1+ix)^2} + \frac{1+(ia)^{\frac{3}{2}}D_1}{(ia)^{\frac{3}{2}}(z_1+ix)^3} + \frac{1}{\sqrt{ia}(z_1-ix)} + \frac{1}{ia(z_1-ix)^2} + \frac{1+(ia)^{\frac{3}{2}}D_2}{(ia)^{\frac{3}{2}}(z_1-ix)^3} \right\}. \quad (33)$$

Using Eqs. (32) and (33),  $Z_{yx}$  in Eq. (20) is written as

$$Z_{yx} = -i\omega \frac{\left\{ \frac{1}{\sqrt{ia}(z_1+ix)} + \frac{1}{ia(z_1+ix)^2} + \frac{1+(ia)^{\frac{3}{2}}D_1}{(ia)^{\frac{3}{2}}(z_1+ix)^3} + \frac{1}{\sqrt{ia}(z_1-ix)} + \frac{1}{ia(z_1-ix)^2} + \frac{1+(ia)^{\frac{3}{2}}D_2}{(ia)^{\frac{3}{2}}(z_1-ix)^3} \right\}}{\left\{ \frac{1}{(z_1+ix)} + \frac{1}{\sqrt{ia}(z_1+ix)^2} + \frac{2+iaC_1}{ia(z_1+ix)^3} + \frac{1}{(z_1-ix)} + \frac{1}{\sqrt{ia}(z_1-ix)^2} + \frac{2+iaC_2}{ia(z_1-ix)^3} \right\}}. \quad (34)$$

In the limit  $x \rightarrow \infty$ , the plane-wave assumption is established

$$Z_{yx} = -\frac{i\omega}{\sqrt{ia}} = \frac{-\sqrt{i\omega}}{\sqrt{\mu_0\sigma_1}}, \quad (35)$$

which is also upheld in the limit  $z_1 \rightarrow -\infty$ . This means that if either the horizontal or vertical distance of the localized current is large enough, the plane-wave assumption remains valid. If this condition is not established, the MT responses would be biased by the source field (see Figs. 1 and 2).

In this study, the focus was on the relationship between the MT responses and the altitude of the source current. The altitude distribution of the conductivity in the ionosphere changes temporally/seasonally

(Sheng et al., 2014), and the region (i.e., E/F) controlling the ionospheric electrical processes also changes temporally (Du and Stening, 1999). Therefore, the altitude of the source current may be considered to vary temporally. Temporal/seasonal changes in the MT responses have been recently well reported (Brändlein et al., 2012; Romano et al., 2014; Vargas and Ritter, 2016; Murphy and Egbert, 2018). These reports are explained by the results in Figs. 1 and 2 because the altitude of the source current varies temporally/seasonally. For example, Romano et al. (2014) reported that, for time periods 20–100 s, the apparent resistivities have a negative correlation with geomagnetic activity. This case indicates an identical polarity with the result in Fig. 1 ( $x = 1$  or 10 km). When the altitude of the source current decreases, the magnetic amplitude increases and the apparent resistivity decreases. As a result, both have a spurious negative correlation.

### **Summary**

In this study, the focus was on the bias in the MT responses due to the variation in altitude of a localized current. The numerical examples show that slight changes in the vertical distance causes a shift in the MT response. In focusing on the source current just above the site, the apparent resistivities/phases have a spurious negative/positive correlation with the magnetic field amplitudes because of changes in the range of altitude of 100–150 km, where the E and F layers exist. These changes in MT responses are seen in real MT data analysis because the vertical distance of the current source varies temporally/seasonally. The temporal changes in MT responses actually reported may be explained by the numerical examples in this study. Considering the range in shift in MT responses, especially at long periods, depends on the vertical distance of the source, we should evaluate the bias due to the source field in real MT-data analysis.

### **Acknowledgements**

The author thanks Dr. Tada-nori Goto, a professor of University of Hyogo, Dr. Katsuaki Koike, a professor of Kyoto University, and Mr. Fumihiko Onoue, a Ph.D. candidate of Scuola Normale Superiore di Pisa, for constructive comments.

### **Reference lists**

- Arfken GB, Weber HJ, Harris FE (2012) *Mathematical methods for physicists: A comprehensive guide*. Academic Press, Cambridge.
- Brändlein D, Lühr H, Ritter O (2012) Direct penetration of the interplanetary electric field to low geomagnetic latitudes and its effect on magnetotelluric sounding. *J Geophys Res: Space Phys* 117(A11). doi:10.1029/2012JA018008.
- Du J, Stening RJ (1999) Simulating the ionospheric dynamo–I. Simulation model and flux tube integrated conductivities. *J Atmos Sol Terr Phys* 61(12): 913-923.

- Häkkinen L, Pirjola R, Sucksdorff C (1989) EISCAT magnetometer cross and theoretical studies connected with the electrojet current system. *Geophysica* 25(1): 123-134.
- Hermance JF, Peltier WR (1970) Magnetotelluric fields of a line current. *J Geophys Res* 75(17): 3351-3356.
- Madden T, Nelson P (1964) A defense of Cagniard's magnetotelluric method. *ONR Rept*: 371-401.
- Murphy BS, Egbert GD (2018) Source biases in midlatitude magnetotelluric transfer functions due to Pc3-4 geomagnetic pulsations. *Earth Planets Space* 70(1).
- Pirjola R (1992) On magnetotelluric source effects caused by an auroral electrojet system. *Radio Sci* 27(04): 463-468.
- Romano G, Balasco M, Lapenna V, Siniscalchi A, Telesca L, Tripaldi S (2014) On the sensitivity of long-term magnetotelluric monitoring in Southern Italy and source-dependent robust single station transfer function variability. *Geophys J Int* 197(3):1425-1441.
- Schmucker U (1970) Anomalies of geomagnetic variations in the southwestern United States. Berkeley: Bull Scripps Inst Oceanogr.
- Sheng C, Deng Y, Yue X, Huang Y (2014) Height-integrated Pedersen conductivity in both E and F regions from COSMIC observations. *J Atmos Sol Terr Phys* 115: 79-86.
- Vargas JA, Ritter O (2016) Source effects in mid-latitude geomagnetic transfer functions. *Geophys J Int* 204(1):606-630.